A NEW WHITE BLOOD CELL SEGMENTATION USING MEAN SHIFT FILTER AND REGION GROWING ALGORITHM

J. Cheewatanon*, **T. Leauhatong***, **S. Airpaiboon***, and **M. Sangwarasilp***,

ABSTRACT

The differential counting of white blood cells (WBCs) provides invaluable information to hematologist for diagnosis and treatment of many diseases. However, manually counting the WBCs is a time-consuming and susceptible to error procedure. Then an automatic and efficient system seems necessary and helpful. In the automatic process, the segmentation of WBC image is one of the most important stages. In this paper, we propose a new algorithm to segment the image. The algorithm consists of two tasks. Firstly, the Mean Shift (MS) filter is used to remove noise. Secondly, we propose a simple but effective region growing algorithm to segment the image. The proposed algorithm was tested in RGB color space and CIE L*a*b* color space, and the experimental results show the excellent performance in both color spaces.

1. INTRODUCTION

There are three types of cells in normal human blood: red blood cells (RBCs), white blood cells (WBCs) and blood platelets. Generally, RBCs are simple and similar. While WBCs contain nucleus and cytoplasm and can be categorized into five classes: Neutrophil, Eosinophil, Basophil, Monocyte and Lymphocyte. Since the number of WBCs in the blood is often an indicator of some diseases such as leukemia and Acquired immune deficiency syndrome (AIDS), the count of different classes of WBC, named Differential Blood Counting (DBC), plays an important role in the determination of the patient health in different stages: diagnosis, treatment, and follow up [1, 2]. In the traditional process, hematologists analyze human blood by microscope. This manual process is time consuming and susceptible to error procedure. Due to the importance of the DBC, an automatic system seems necessary and helpful. The automatic DBC system may require four stages: 1) acquisition, 2) detection, 3) feature extraction, and 4) classification. In the first stage, the blood smear is magnified to a suitable scale under the microscope, and then transformed to a digital image. In the second stage, cell segmentation is used to produce a number of single-cell images. Then each single-cell image is segmented into three regions: 1) nucleus, 2) cytoplasm, and 3) background. In the third step, feature vectors of color, texture, and shape of the segmented cell and its nucleus are extracted. In the last step according to the extracted feature vectors, each WBC is labeled by a classifier. The most important stage is the cell segmentation because the accuracy of segmentation plays a crucial role in the subsequent stages [3-5]. Unfortunately, the microscopic blood image always has staining reagent and illumination inconsistencies. Besides, the maturity classes of the white blood cells actually represent a continuum, cells frequently overlap each other, and there is fairly wide variation of size and shape of nuclear and cytoplasmic regions within given cell classes. Such difficulties make the WBC segmentation a hard and challenging problem. There are a number of cell segmentation algorithms available. For example, Shitong and Min introduced a new detection algorithm which combines the advantage of Threshold Segmentation followed by Mathematical Morphology (TSMM) and Fuzzy Cellular Neural Network (FCNN) to detect the WBC [6]. However, to reduce the computational time, the hardware implementation is required. Then it is expensive and inconvenient in some applications. Next, active contour techniques were proposed to extract boundaries of WBC [1, 7, 8]. The active contour based segmentation requires the initial contour of the convex hull of the nucleus boundary which is also the problem of cell segmentation. Then the fully automatic approaches of the active contour based techniques are difficult to implement. In this paper, we propose a new algorithm to segment a WBC from a color microscopic blood image. The proposed algorithm is based on two assumptions. The first assumption is that the WBC images can be represented as a set of regions whose observed colors change slowly, but they change abruptly when across the boundary between the regions. However in the real-world application, the observed colors in a given region can change unexpectedly due to the fact that the images are always contaminated by noise. To solve this problem, the second assumption is proposed. The assumption is

Manuscript received on April 5, 2011.,

Department of Electronics, Faculty of Engineering, King Mongkuts Institute of Technology Ladkrabang, Thailand

based on the fact that, in practical application, the boundaries of the regions are not destroyed by noise. Then the second assumption is that the size of the abrupt change at the boundary is always bigger than the size of the unexpected change by noise. The proposed algorithm is designed as follows. According to the second assumption, the image is filtered by the mean shift (MS) filter which is an effective edge-preserving filter. Barash and Comaniciu showed that the MS filter outperforms other edge-preserving filters including Nonlinear Diffusion and Bilateral filter [9]. The MS filter is an iterative algorithm to detect local mode in the joint spatial-range domain. It can filter noise while preserve the boundary by choosing a suitable bandwidth of spatial and range part. Next, the filtered image is segmented by using a new region growing algorithm. In this paper, a simple but effective region growing algorithm based on the first assumption is proposed. Furthermore, the proposed algorithm was tested in RGB color space and CIE L*a*b* color space. The rest of the paper is organized as follows. Section 2 is devoted to the theories of CIE L*a*b* color space, MS filter, and the region growing algorithm. The experiments of the proposed algorithm are shown in Section 3. The paper is concluded and the future work is indicated in Section 4..

2. THEORIES

2.1 CIE L*a*b* Color Space

The RGB color space can be transformed to the CIE L*a*b* color space [10] as follows:

$$\begin{bmatrix} X \\ Y \\ Z \end{bmatrix} = \frac{100}{255}\times \begin{bmatrix} 0.41253 & 0.357580 & 0.180423 \\ 0.212671 & 0.715160 & 0.072169 \\ 0.019334 & 0.119193 & 0.950227 \end{bmatrix} \times \begin{bmatrix} R \\ G \\ B \end{bmatrix} \quad (1)$$

$$L^* = 116 f\left(\frac{Y}{Y_0}\right) - 16,$$

$$\mathrm{a}^* = 500\left[f\left(\frac{X}{X_0}\right) - f\left(\frac{Y}{Y_0}\right)\right],$$

$$\mathrm{b}^* = 200\left[f\left(\frac{Y}{Y_0}\right) - f\left(\frac{Z}{Z_0}\right)\right], \quad (2)$$

where $R, G, B \in [0, 255]$. X_0, Y_0 and Z_0 are the tristimulus values of the reference white. In real applications of the WBC, information of reference whites of images in database can not be available, and the CIE day-light illuminant D65 is commonly used in digital cameras. Therefore, we set $X_0 = 95.047$, $Y_0 = 100$ and $Z_0 = 108.883$ [10]. The function $f(q)$ is defined by:

$$\mathrm{f}(q) = \begin{cases} \sqrt[3]{q}, & (q > 0.008856) \\ 7.787q, & (q < 0.008856) \end{cases}$$

2.2 Mean Shift Filter

Let $X = \{x_i\}_{i=1}^n$ be a set of n data points in d-dimensional space, R^d. The multivariate kernel density estimator with Gaussian kernel and a symmetric positive definite $d \times d$ bandwidth matrix H, computed at the point x is given by

$$\hat{f}(x) = \frac{1}{n\,|2\pi H|^{\frac{1}{2}}} \sum_{i=1}^{n} \exp(-\frac{1}{2} d^2(x, x_i, H)) \quad (3)$$

where

$$d^2(x, x_i, H) \equiv (x - x_i)^T H^{-1} (x - x_i), \quad (4)$$

is the Mahalanobis distance from x to x_i. By computing the gradient of $\hat{f}(x)$

$$\nabla \hat{f}(x) = \frac{H^{-1}}{n\,|2\pi H|^{\frac{1}{2}}} \sum_{i=1}^{n} (x_i - x) \times \exp\left(-\tfrac{1}{2} d^2(x, x_i, H)\right) \quad (5)$$

after some algebra we have

$$m(x) = H \frac{\nabla \hat{f}(x)}{\hat{f}(x)}, \quad (6)$$

where

$$m(x) = \frac{\sum_{i=1}^{n} x_i \exp\left(-\frac{1}{2} d^2(x, x_i, H)\right)}{\sum_{i=1}^{n} \exp\left(-\frac{1}{2} d^2(x, x_i, H)\right)} - x, \quad (7)$$

is the mean shift vector.

Assume now that the data points x_i are extracted from an input image. Then the vector components of x_i contain both the spatial lattice information $x_{si} = (x_i, y_i)^T$ and range information $x_{ci} = (c_{i1}, c_{i2}, c_{i3})^T$ where c_{i1}, c_{i2} and c_{i3} are three color components at position (x_i, y_i). Then $x_i = (x_{si}^T, x_{ri}^T)^T$ is a data point in joint spatial-range domain. We assume that the bandwidth matrix H is diagonal having the diagonal terms equal to σ_S^2 for the spatial part and σ_R^2 for the range part. Then the Mahalanobis distance in Equ. (4) can be rewritten as:

$$d^2(x, x_i, H) \equiv \frac{\|x_s - x_{si}\|^2}{2\sigma_S^2} + \frac{\|x_r - x_{ri}\|^2}{2\sigma_R^2} \quad (8)$$

where

$$\|x_s - x_{si}\|^2 \equiv (x - x_i)^2 + (y - y_i)^2 \quad (9)$$

Moreover, the color distance in the RGB space is defined as,

$$\|x_r - x_{ri}\|^2 \equiv (r - r_i)^2 + (g - g_i)^2 + (b - b_i)^2 \quad (10)$$

and the color distance in the CIE L*a*b* space is defined as,

Table 1: *The MS Filter Algorithm*

1.	Set t=0, and initial the error ε
2.	Set $y_i^0 = x_i$ for $i = 1, ..., n$.
3.	Calculate the convergent value $y_i^{'}$ for $i = 1, ..., n$. by 3.1 Update $y_i^{t+1} = \frac{\sum_{i=1}^{n} x_i \exp\left(-\frac{1}{2} d^2\left(y_i^t, x_i, H\right)\right)}{\sum_{i=1}^{n} \exp\left(-\frac{1}{2} d^2\left(y_i^t, x_i, H\right)\right)}$ 3.2 if $d^2(y_i^t, y_i^{t+1}, H) > \varepsilon$ go to step 3.1
4.	Set $zi = (x_{si}^T, y_{ri}^{'T})$, where $y_{ri}^{'}$ is the range part of the convergent value $y_i^{'}$.

$$\|x_r - x_{ri}\|^2 \equiv (L^* - L_i^*)^2 + (a^* - a_i^*)^2 + (b^* - b_i^*)^2 \quad (11)$$

The MS filter is an iterative algorithm for local mode detection in the joint spatial-range domain, and can be formulated as follows. Let $Y = \{y_i\}_{i=1}^n$ and $Z = \{z_i\}_{i=1}^n$ be a set of data points in joint spatial-range domain of the processed data and the result filtered image respectively. The MS filter is formulated as shown in Table 1., and can be explained as follows. Each data point y_i is initialized at x_i and, during calculating the convergent in step 3.1 and 3.2, y_i moves iteratively along the gradient direction in both spatial and range domain. Finally, it converges to the nearest local mode in the joint spatial-range domain. Finally, the colors of the filtered image are set to the colors of the nearest local mode in spatial-range domain. The advantage of the MS filter is that the image structure does not change during iterations [8]. Then the MS filter will achieve better image structure preservation. The MS filter can remove noise while preserving edges or boundaries of the local structure by choosing the suitable values of σ_S^2 and σ_R^2.

2.3 Region Growing Algorithm

Given a data point of the filtered image, $z = \left((x, y)^T, (y)_r^{'T}\right)$, its four neighbors are defined as follows:

$$z_0 = \left((x-1, y)^T, (y)_{r0}^{'T}\right),$$
$$z_1 = \left((x+1, y)^T, (y)_{r1}^{'T}\right),$$
$$z_2 = \left((x, y-1)^T, (y)_{r2}^{'T}\right),$$
$$z_3 = \left((x, y+1)^T, (y)_{r3}^{'T}\right) \quad (12)$$

On the other hand, z is called the center of its neighbors.

Let $L = \{1, 2, ...\}$ be a set of labels of regions, and the unlabeled regions is labeled as 0. According to the first assumption, the Region growing algorithm is designed as follows. Given a data point z which is labeled as $Idx (Idx \in L)$ its neighbors are also labeled as , Idx if $\left\| y_r^{'T} - y_{ri}^{'T} \right\|^2 \sigma_R^2$. A recursive growing function, called RegionGrow(z, z_i, Idx), is defined as shown in Table 2.

Table 2: *The Schematic of RegionGrow* (z, z_i, Idx)

1.	If $\left\| y_r^{'T} - y_{ri}^{'T} \right\| > \sigma_R^2$ then return.
2.	If z_i is not labeled as 0, then return
3.	Label z_i as Idx
4.	Recursively call RegionGrow(z_i, z_{i0}, Idx), RegionGrow(z_i, z_{i1}, Idx), RegionGrow(z_i, z_{i2}, Idx) and RegionGrow(z_i, z_{i3}, Idx),
5.	Return

Moreover, the main program of the Region growing algorithm is defined as shown in Table 3

Table 3: *The Main Program*

1.	Label all data points as 0.
2.	Set $Idx = 1$.
3.	Search an unlabeled z from the filtered image.
4.	Label z as Idx.
6.	Call RegionGrow(z, z_i, Idx).
5.	Set $Idx = Idx + 1$.
6.	If the unlabeled data points still exist, then go to step 3.

3. EXPERIMENTS

3.1 The Experiments in RGB Color Space

The experiments of mean shift filter in RGB color space and the segmentation by using the proposed region growing algorithm of Basophil, Eosinophil, Lymphocyte, Monocyte, and Neutrophil are shown in Fig. 1-5 respectively.

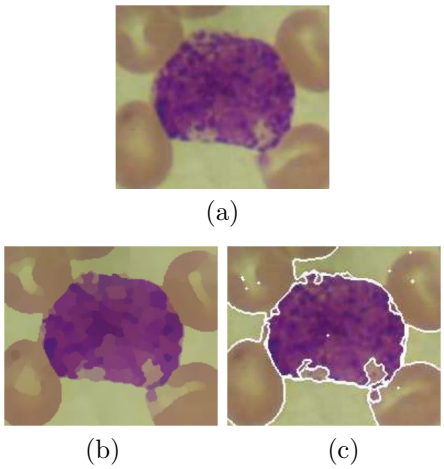

(a)

(b) (c)

Fig.1: *The Segmentation Experiments of Basophil. (a)The original image (b)The MS filtered image with* $\sigma_S^2 = 9, \sigma_R^2 = 100$ *(c)The segmented image*

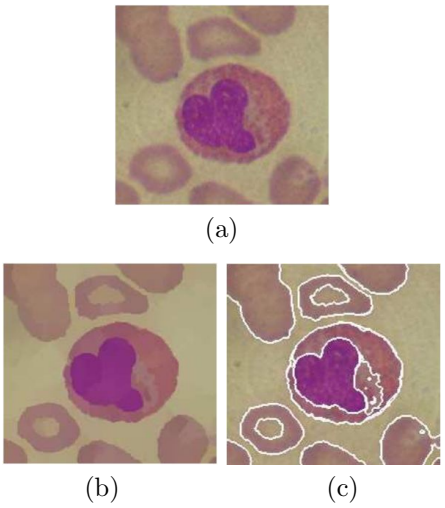

Fig.2: *The Segmentation Experiments of Eosinophil. (a)The original image (b)The MS filtered image with* $\sigma_S^2 = 25.00, \sigma_R^2 = 42.25$ *(c)The segmented image*

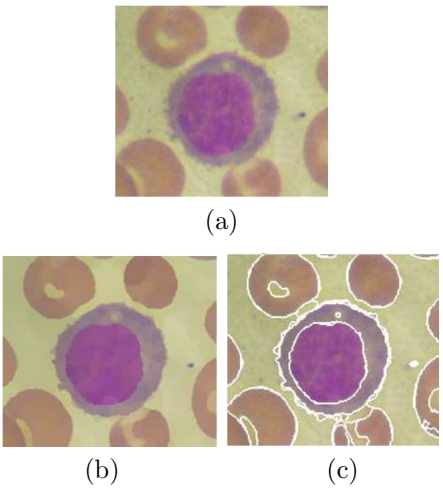

Fig.3: *The Segmentation Experiments of Lymphocyte. (a)The original image (b)The MS filtered image with* $\sigma_S^2 = 12.25, \sigma_R^2 = 42.25$ *(c)The segmented image*

As shown in Fig. 1-5, all classes of white blood cells can be segmented in RGB space by using the proposed algorithm effectively. It can be seen from the filtered images that noise can be removed, while edges can be preserved effectively. Also, the sharpness at the boundaries is higher than the original image. Next, the nucleuses and cytoplasm can be segmented by using the proposed region growing algorithm. However, many over-segmented region can be seen in the cytoplasm region. Finally, it can be seen that the effectiveness of the segmented images highly depends on the selected bandwidth.

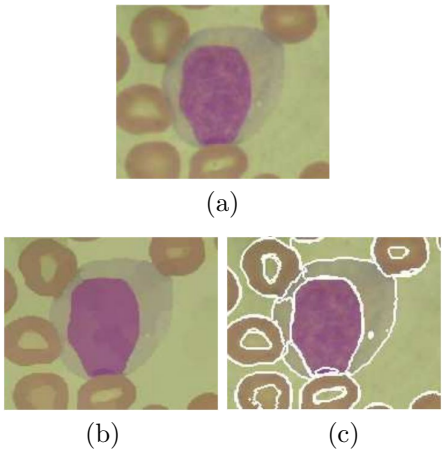

Fig.4: *The Segmentation Experiments of Monocyte. (a)The original image (b)The MS filtered image with* $\sigma_S^2 = 25, \sigma_R^2 = 25$ *(c)The segmented image*

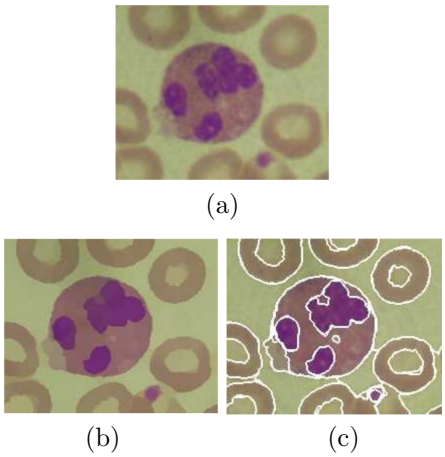

Fig.5: *The Segmentation Experiments of Neutrophil. (a)The original image (b)The MS filtered image with* $\sigma_S^2 = 42.25, \sigma_R^2 = 16$ *(c)The segmented image*

3.2 The Experiments in CIE L*a*b* Color Space

The experiments of mean shift filter in CIE L*a*b* color space and the segmentation by using the proposed region growing algorithm of Basophil, Eosinophil, Lymphocyte, Monocyte, and Neutrophil are shown in Fig. 6-10 respectively.

As shown in Fig. 6-10, all classes of white blood cells can be segmented in CIE L*a*b* color space effectively. Moreover, the number of over-segmented region is reduced.

4. CONCLUSION AND FUTURE WORKS

The experimental results show that the MS filter can successfully remove noise from the WBC images while preserving the edges. Moreover, the sharpness of the boundaries of the filtered image is enhanced. In cases of the RGB color space, the white blood cell

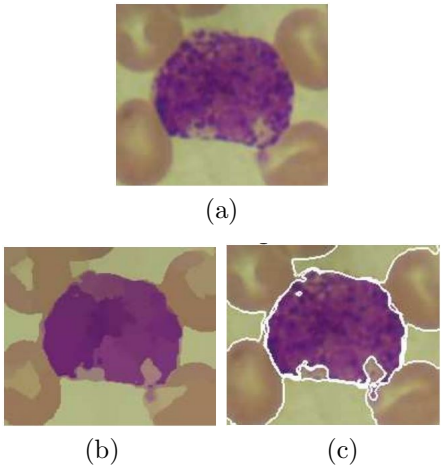

Fig.6: *The Segmentation Experiments of Basophil. (a)The original image (b)The MS filtered image with* $\sigma_S^2 = 49, \sigma_R^2 = 25$ *(c)The segmented image*

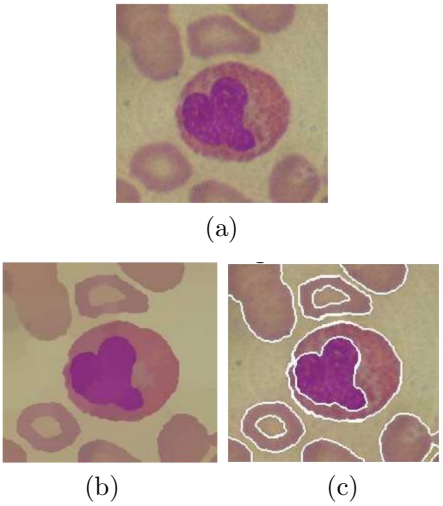

Fig.7: *The Segmentation Experiments of Eosinophil. (a)The original image (b)The MS filtered image with* $\sigma_S^2 = 46.24, \sigma_R^2 = 12.96$ *(c)The segmented image*

images can be segmented by using the proposed algorithm, but the segmented images are highly over-segmented in the cytoplasm region. On the other hand, the over-segmented region can be reduced by using the CIE L*a*b* color space. Finally, it can be seen that the effectiveness of the segmented images highly depends on the selected bandwidth. In the future works, an automatic method of selecting the suitable bandwidth must be developed.

References

[1] G. Ongun, U. Halici, K. Leblebicioglu, V. Atalay, M. Beksac, S. Beksac, *Feature Extraction and Classification of Blood Cells for an Automated Differential Blood Count System,* International Joint Conference on Neural Networks, 2001, vol. 4, pp.

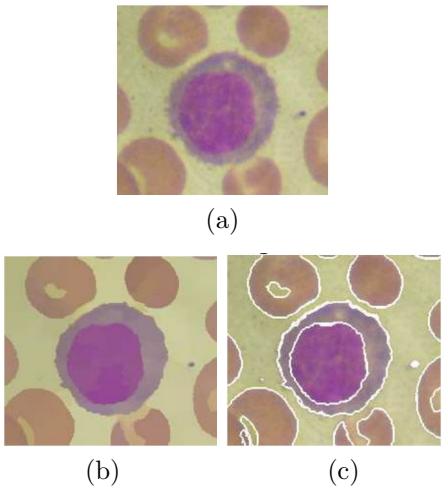

Fig.8: *The Segmentation Experiments of Lymphocyte. (a)The original image (b)The MS filtered image with* $\sigma_S^2 = 38.44, \sigma_R^2 = 17.64$ *(c)The segmented image*

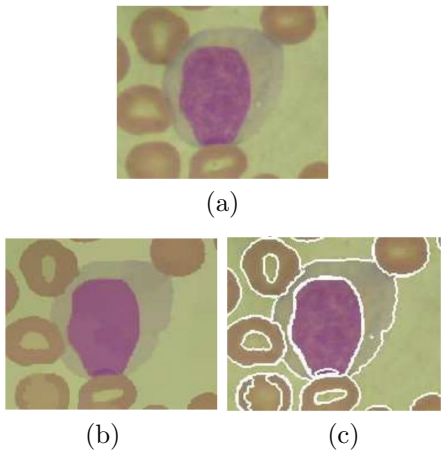

Fig.9: *The Segmentation Experiments of Monocyte. (a)The original image (b)The MS filtered image with* $\sigma_S^2 = 46.24, \sigma_R^2 = 10.24$ *(c)The segmented image*

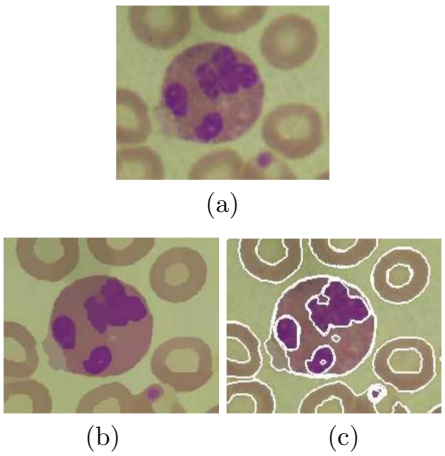

Fig.10: *The Segmentation Experiments of Neutrophil. (a)The original image (b)The MS filtered image with* $\sigma_S^2 = 33.64, \sigma_R^2 = 9.00$ *(c)The segmented image*

2461-2466, 2001.

[2] N. Theera-Umpon, *White Blood Cell Segmentation and Classification in sMicroscopic Bone Marrow Images,* Lecture Notes in Computer Science, vol. 3614, pp. 787796, August 2005.

[3] B.R. Kumar, D.K. Joseph, and T.V. Sreenivas, *Teager Energy Based Blood Cell Segmentation,* International Conference on Digital Signal Processing, vol. 2, pp. 619-622, 2002.

[4] E. Montseny, P. Sobrevilla, and S. Romani, *A Fuzzy Approach to White Blood Cells Segmentation in Color Bone Marrow Images,* IEEE Conference on Fuzzy Systems, 2004, vol. 1, pp. 173-178, 2004.

[5] W. Shitong and W. Min, *A New detection Algorithm (NDA) Based on Fuzzy Cellular Neural Networks for White Blood Cell Detection,* IEEE Trans. on Information Technology in Biomedicine, vol. 10, iss. 1, pp. 5-10, 2006.

[6] F. Zamani and R. Safabakhsh, *An Unsupervised GVF Snake Approach for White Blood Cell Segmentation Based on Nucleus,* ICSP, 2006.

[7] A. Sanpanich, W. Iampa, C. Pintavirooj, and P. Tosranon, *White Blood Cell Segmentation by Distance Mapping Active Contour*, International Symposium on Communications and Information Technologies, ISCIT 2008, October 2008.

[8] D. Barash and D Comaniciu, *A Common Framework for Nonlinear Diffusion, Adaptive Smoothing, Bilateral Filtering, and Mean Shift,* Image and Video Computing, vol. 22, no. 1, pp. 73-81, Jan., 2004.

[9] *Recommendations on Uniform Color Spaces, Color Difference Equations, Psychometric Color Terms*, C.I.E. Supplement No. 2 to CIE publication no. 15(E-131) 1971/(TC-1.3) 1978.

Jidtrawadee Cheewatanon received the B.Eng. Degrees with second rank honor in Electronics Engineering from King Mongkut's Institute of Technology in 2005. Her research interests are embedded system, medical image processing.

Thurdsak Leauhatong received the B.Eng. degrees in Electronics Engineering, and M.Eng. degree in Electrical Engineering from King Mongkut's Institute of Technology Ladkrabang, Thailand in 1992 and 1997, respectively, and doctoral degree in Science and Technology from Tokai University, Japan. His research interests are content-based image retrieval, vector quantization, and medical image processing.

Surapan Airpaiboon received the B.S.c (Physics) from Naresuan University in 1987, M. Eng. in Electrical Engineering, from King Mongkut's Institute of Technology in 1990, and D. Eng. in Electrical Engineering in 1998 from Tokai University, Japan. His research interests are signal and image processing.

Manas Sangwarasilp received the B.Eng. degree from King Mongkut's Institute of Technology Ladkrabang (KMITL), Bangkok, in 1973, and the M.Eng. degree and D.Eng. in telecommunications from Tokai University, Tokyo, Japan, in 1977 and 1991, respectively.

From 2003 to 2007, he was the Director of Computer Research and Service Center, KMITL, where he is currently and Associate Professor with the Faculty of Engineering, Department of Electronics. His current research interests include image reconstruction, 3-D modeling, image classification, and image filtering.

He was a member of the Advising Committee of the Thai Biomedical Engineering Research Association, the Chairman of the 1st Symposium on Thai Biomedical Engineering (ThaiBME 2008), and the Chairman of the 30th Electrical Engineering Conference (EECON-30)